

Modeling Photon Propagation In Anisotropically Scattering Media With The Equation Of Radiative Transfer

Alexander D. Klose and Andreas H. Hielscher

Departs. of Biomedical Engineering & Radiology, Columbia University, ET351 Mudd Building,
MC 8904, 500 West 120th Street, New York, N.Y. 10027, USA

ABSTRACT

The equation of radiative transfer can take into account the anisotropic scattering behavior of photons and anisotropic sources for modeling the light propagation in tissue. This is an important aspect when small tissue geometries are considered. In this case the solutions of the commonly applied diffusion approximation may provide only insufficiently accurate results. We numerically solve the equation of radiative transfer by means of a finite-difference discrete-ordinates technique. However, strong anisotropically scattering media require many discrete ordinates, which lead to a large computational burden. In this study we implemented a Delta-Eddington method that allows using only a small number of discrete ordinates, and the solution can be obtained at a lesser computational costs.

Keywords: equation of radiative transfer, discrete-ordinates method, Delta-Eddington method, anisotropic scattering, anisotropic source, phase function, tissue optics

1. INTRODUCTION

The propagation of photons in biological tissue can be accurately described with the equation of radiative transfer (ERT). An accurate description of light transport is important for model-based iterative image reconstruction (MOBIIR) schemes commonly used in optical tomography (OT).^{1,2} Within these schemes light propagation models are employed for predicting detector readings on the tissue boundary as a function of absorption and scattering coefficients inside the tissue.

Most light propagation models in OT are based on the diffusion equation, which is an approximation to the ERT. The diffusion approximation has limited applicability in highly absorbing media, media with low-scattering regions, and media with small geometries where boundary effects are dominating.³⁻⁹ Furthermore, problems with this approximation have been reported when anisotropic sources are used.^{3,6,8} We present in this work numerical simulations that show light distributions in turbid media as a function of anisotropic scattering and the anisotropy of the source. In addition we investigated how the medium size affects the results. Similar studies have already been performed for transient short-pulse radiative transfer in anisotropic scattering planar media using a Monte-Carlo method¹⁰ and for highly absorbing media with small source-detector separations based on a generalized diffusion approximation.⁶ Studies have not been carried out, however, for the time-independent ERT using a finite-difference discrete-ordinates method.

All numerical calculations in this work are done with a finite-difference discrete-ordinates method. The numerical determination of a solution of the ERT becomes computationally very time-consuming for typical anisotropy factors of biological tissue. Therefore, we have implemented a Delta-Eddington method that considerably reduces the time of the solution process.

Further author information:

A.D.K.: E-mail: ak2083@columbia.edu, Telephone: 1 212 854 5868

A.H.H.: E-mail: ahh2004@columbia.edu, Telephone: 1 212 854 5080

2. THEORY

2.1. Equation Of Radiative Transfer

The photon transport in tissue can be mathematically described by the particle transport equation. This is a balance equation for the angular flux of photons, called radiance. A derivation of this equation is given by Duderstadt and Martin.¹¹ The particle transport equation applied to photons is also called equation of radiative transfer.¹¹ The time-independent ERT in a three-dimensional spatial domain is given by:

$$\mathbf{\Omega} \cdot \nabla \psi(\mathbf{r}, \mathbf{\Omega}) + (\mu_a(\mathbf{r}) + \mu_s(\mathbf{r}))\psi(\mathbf{r}, \mathbf{\Omega}) = S(\mathbf{r}, \mathbf{\Omega}) + \mu_s(\mathbf{r}) \int_{4\pi} p(\mathbf{\Omega}, \mathbf{\Omega}')\psi(\mathbf{r}, \mathbf{\Omega}')d\mathbf{\Omega}'. \quad (1)$$

The fundamental quantity in radiative transport theory is the radiance $\psi(\mathbf{r}, \mathbf{\Omega})$, with units of $\text{Wcm}^{-2}\text{sr}^{-1}$, at the spatial position \mathbf{r} and unit direction $\mathbf{\Omega}$. The spatial position and the direction of the radiance are defined by means of two coordinate systems.¹¹ A *laboratory coordinate system* describes the geometry of the medium in three-dimensional space. Each point of the medium is denoted by a vector $\mathbf{r} = \mathbf{r}(x, y, z)$ in *Cartesian* coordinates. Furthermore, a *local coordinate system* describes the local scattering process of light along directions $\mathbf{\Omega}$ at a particular point \mathbf{r} . The local coordinate system can be expressed in spherical coordinates with $\mathbf{\Omega} = \mathbf{\Omega}(\vartheta, \varphi)$. Both coordinate systems are shown in figure (1).

Furthermore, the integral of the radiance $\psi(\mathbf{r}, \mathbf{\Omega})$ over all directions $\mathbf{\Omega}$ at one point \mathbf{r} yields the fluence $\phi(\mathbf{r})$ with units of Wcm^{-2} :

$$\phi(\mathbf{r}) = \int_{4\pi} \psi(\mathbf{r}, \mathbf{\Omega})d\mathbf{\Omega}. \quad (2)$$

Other quantities besides the radiance ψ that are included in the ERT are the source term $S(\mathbf{r}, \mathbf{\Omega})$ with the unit $\text{Wcm}^{-3}\text{sr}^{-1}$, the scattering coefficient, $\mu_s(\mathbf{r})$, the absorption coefficient, $\mu_a(\mathbf{r})$, both given in units of cm^{-1} , and the scattering phase function $p(\mathbf{\Omega}, \mathbf{\Omega}')$ with units of sr^{-1} .

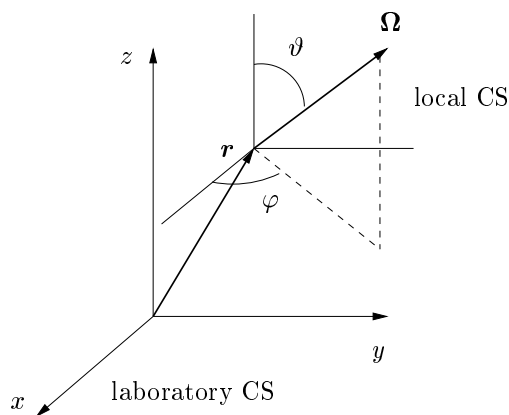


Figure 1. The laboratory coordinate system describes the global geometry of the scattering medium that contains all points \mathbf{r} . The local coordinate system describes the local scattering process into directions $\mathbf{\Omega}$ at the point \mathbf{r} .

2.2. Finite-Difference Discrete-Ordinates Method

The direction $\mathbf{\Omega}$ in the ERT is replaced with a set of discrete ordinates $\mathbf{\Omega}_k$ by utilizing a *discrete ordinates* (S_N) method.^{12, 13} The integral in the ERT is approximated with a quadrature rule

$$\int_{4\pi} p(\mathbf{\Omega}, \mathbf{\Omega}')\psi(\mathbf{\Omega}')d\mathbf{\Omega}' \approx \sum_{k'=1}^K w_{k'} p(\mathbf{\Omega}_k, \mathbf{\Omega}_{k'})\psi(\mathbf{\Omega}_{k'}) \quad (3)$$

where w_k are appropriate weights determined by *full level symmetry* of the ordinates.¹³ The total number of ordinates K is given by $K = \mathcal{N}(\mathcal{N} + 2)$ with \mathcal{N} the number of direction cosines of the $S_{\mathcal{N}}$ method. The angular discretization yields a set of K coupled differential equations for the radiance $\psi(\mathbf{r}, \mathbf{\Omega}_k) = \psi_k(\mathbf{r})$ in the directions $\mathbf{\Omega}_k$. The spatial derivatives of the ERT are replaced with a finite-difference scheme. In this work we use an upwind-difference scheme. The upwind-difference formula depends on the directions $\mathbf{\Omega}_k$ of the angular-dependent radiance $\psi_k(\mathbf{r})$. The resulting algebraic system of equations is solved with a *Gauss-Seidel method*.¹⁴⁻¹⁶

2.3. Scattering Phase Function

The scattering phase function $p(\mathbf{\Omega}, \mathbf{\Omega}')$ describes the anisotropic scattering behavior of photons in biological tissue. In tissue optics this function is typically assumed to be independent of \mathbf{r} . The phase function gives the probability that a single photon is deflected by an angle θ . The angle θ encloses the two directions formed by $\mathbf{\Omega}$ and $\mathbf{\Omega}'$ in the interval $\theta \in [0, \pi]$ with $\mathbf{\Omega} \cdot \mathbf{\Omega}' = \cos \theta$. Furthermore, the phase function p is normalized with

$$\int_{4\pi} p(\mathbf{\Omega}, \mathbf{\Omega}') d\mathbf{\Omega}' = \int_{4\pi} p(\mathbf{\Omega} \cdot \mathbf{\Omega}') d\mathbf{\Omega}' = \int_{4\pi} p(\cos \theta) d\mathbf{\Omega}' = 2\pi \int_{-1}^1 p(\cos \theta) d\cos \theta = 1. \quad (4)$$

The expectation value of $\cos \theta$ with

$$g = \langle \cos \theta \rangle = 2\pi \int_{-1}^1 \cos \theta p(\cos \theta) d\cos \theta \quad (5)$$

is called the anisotropy factor g .

A commonly applied scattering phase function in tissue optics is the Henyey-Greenstein (HG) phase function p_{HG} ^{17, 18} and is given as

$$p_{HG}(\cos \theta) = \frac{1 - g^2}{4\pi(1 + g^2 - 2g \cos \theta)^{3/2}}. \quad (6)$$

This function can also be expanded into a series of Legendre polynomials $P_n(\cos \theta)$

$$p_{HG}(\cos \theta) = \frac{1}{4\pi} \sum_{n=0}^N (2n + 1) b_n P_n(\cos \theta) \quad (7)$$

with the coefficients

$$b_n = \int_{4\pi} p_{HG}(\cos \theta) P_n(\cos \theta) d\mathbf{\Omega} = 2\pi \int_{-1}^1 p_{HG}(\cos \theta) P_n(\cos \theta) d\cos \theta = g^n. \quad (8)$$

An isotropic scattering medium is described by $b_0 = 1$ and $b_n = 0$. The anisotropy factor g in equation (6) equals the coefficient $b_1 = g$ for anisotropically scattering media.⁷

For highly anisotropically scattering media ($g > 0.8$) the computational burden becomes very large. Many Legendre polynomials and discrete ordinates are needed to account for a sufficiently accurate angular discretization. If the number of used discrete ordinates K is too small, the condition (see equation (4)) for a normalized phase function is not satisfied anymore:

$$\sum_{k'=1}^K w_{k'} p(\mathbf{\Omega}_k, \mathbf{\Omega}_{k'}) \neq 1. \quad (9)$$

That leads to false scattering and affects the accuracy of the discrete-ordinates technique.¹⁹

2.4. Delta-Eddington Method

The Delta-Eddington method²⁰ reduces the number of discrete ordinates and Legendre polynomials by transforming the phase function into two separate terms:^{21,22}

- a fraction f of scattered photons within a collimated laser beam is described by a δ -function and
- another fraction $(1 - f)$ out of the collimated laser beam scattered photons is described by a new HG phase function p'_{HG}

$$p_{HG}(\cos \theta) \approx p_{\delta-HG}(\cos \theta) = (1 - f)p'_{HG}(\cos \theta) + \frac{1}{2\pi}f\delta(1 - \cos \theta). \quad (10)$$

The HG phase function $p'_{HG}(\cos \theta)$ is also expanded into a series of Legendre polynomials:

$$p'_{HG}(\cos \theta) = \frac{1}{4\pi} \sum_{n=0}^N (2n + 1)b'_n P_n(\cos \theta). \quad (11)$$

Substitution of the HG phase function (equation (6)) into equation (10) and replacing the δ -function with a series of Legendre polynomials gives the new coefficients²¹

$$b'_n = \frac{b_n - f}{1 - f} \text{ with } f = g^{N+1}. \quad (12)$$

N denotes the number of terms after the series expansion in equation (11) is terminated. The ERT can now be re-written by inserting equation (10) into equation (1)

$$\boldsymbol{\Omega} \cdot \nabla \psi(\mathbf{r}, \boldsymbol{\Omega}) + (\mu_a + (1 - f)\mu_s)\psi(\mathbf{r}, \boldsymbol{\Omega}) = S(\mathbf{r}, \boldsymbol{\Omega}) + (1 - f)\mu_s \int_{4\pi} p'_{HG}(\boldsymbol{\Omega}, \boldsymbol{\Omega}')\psi(\mathbf{r}, \boldsymbol{\Omega}')d\boldsymbol{\Omega}'. \quad (13)$$

3. RESULTS

3.1. Problem Set-Up

We studied the differences in the fluence distributions of isotropic scattering media ($\phi^{g=0}(\mathbf{r})$) and anisotropic scattering media ($\phi^{g=0.95}(\mathbf{r})$) as a function of the medium size. This study was performed for either a diffusively light-emitting (isotropic) source S^{dif} or a collimated (anisotropic) source S^{col} . A diffuse source S^{dif} emitted light into the angular half-space 2π sr since the source was positioned on the medium boundary, whereas the collimated source S^{col} covered an angle of $\approx 0.33\pi$ sr that was forward-peaked into the medium. In addition, we performed calculations for the fluence distributions $\phi^{dif}(\mathbf{r})$ and $\phi^{col}(\mathbf{r})$ by using either a diffuse source S^{dif} or a collimated source S^{col} . This study was performed in isotropically ($g = 0$) and anisotropically ($g = 0.95$) scattering media as a function of the medium size.

The media under consideration had different geometrical dimensions (1 cm \times 1 cm, 2 cm \times 2 cm, 4 cm \times 4 cm, and 8 cm \times 8 cm). Therefore, our numerical domain was varied with grid points 41 \times 41, 81 \times 81, 161 \times 161, and 321 \times 321 since the spatial step size of adjacent grid points was kept constant with $\Delta x = \Delta y = 0.025$ cm. The reduced scattering coefficient $\mu'_s = (1 - f)\mu_s = 10$ cm⁻¹ and the absorption coefficient $\mu_a = 0.2$ cm⁻¹ were constant for all simulations. Note that in this case ($\mu'_s \gg \mu_a$) it is generally assumed that the diffusion approximation is valid. Since we simulated isotropically ($g = 0$) and anisotropically ($g = 0.95$) scattering media we had to adjust the scattering coefficient μ_s according to equation $\mu'_s = (1 - f)\mu_s$ with $f = g^3$ ($N = 2$ in equation (12)). For an isotropically scattering medium we obtained the following set of optical parameters $\{g = 0, \mu_s = 10$ cm⁻¹ $\}$, and for the anisotropically scattering medium we had $\{g = 0.95, \mu_s = \mu'_s/(1 - f) = 28.52$ cm⁻¹ $\}$. The calculations were carried out with a S_6 method (48 discrete ordinates). The fluence distributions were normalized to the source term on the medium boundary with the condition

$$\int_{4\pi} S^{dif}(\mathbf{r}, \boldsymbol{\Omega})d\boldsymbol{\Omega} = \int_{4\pi} S^{col}(\mathbf{r}, \boldsymbol{\Omega})d\boldsymbol{\Omega} = const. \quad (14)$$

The differences of the fluence distributions are expressed by the ratios $\phi^{g=0.95}/\phi^{g=0}$ for different sources, and ϕ^{col}/ϕ^{dif} for different anisotropy factors.

3.2. Diffuse Sources In Media With Different Anisotropy Factors

We calculated the fluence distributions $\phi^{g=0.95}$ and $\phi^{g=0}$ for media with an anisotropy factor $g = 0.95$ and $g = 0$. The source term constituted a diffuse source S^{dif} that was placed on the center top boundary of the medium. As can be seen in figure (2) the ratio of both light distributions is in the range of 0.975 to 1.025 for most areas in all 4 media. Therefore, $\phi^{g=0.95}$ is almost identical to $\phi^{g=0}$. This result is also in accordance with the diffusion approximation, where the scattering coefficient μ_s of a highly anisotropically scattering medium ($g = 0.95$) can be replaced with a reduced scattering coefficient $\mu'_s = (1 - f)\mu_s$ of an isotropically scattering medium ($g = 0$) yielding the same results for the fluence distributions $\phi^{g=0.95}$ and $\phi^{g=0}$.

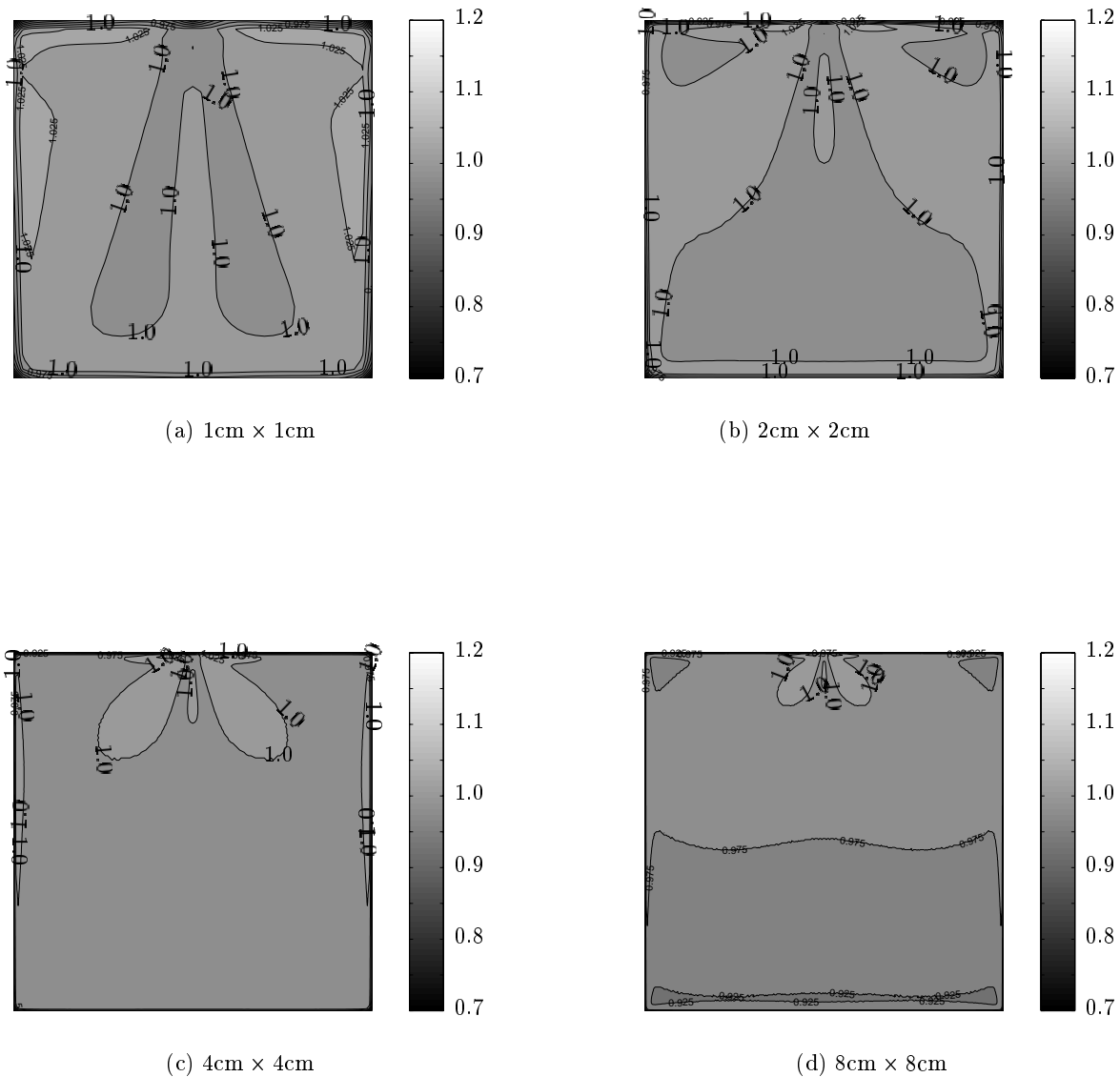


Figure 2. Ratios $\phi^{g=0.95}/\phi^{g=0}$ for different media sizes: (a) 1cm \times 1cm, (b) 2cm \times 2cm, (c) 4cm \times 4cm, (d) 8cm \times 8cm. A diffuse source S^{dif} was placed at the top center of the medium boundary.

3.3. Collimated Sources In Media With Different Anisotropy Factors

In a second example, we calculated the fluence distributions for anisotropically ($g = 0.95$) and isotropically ($g = 0$) scattering media using a collimated source S^{col} as can be seen in figure (3). The fluence distribution $\phi^{g=0.95}$ of the anisotropically scattering medium deviates from the isotropically scattering medium by a factor of 1.2 in the vicinity of the collimated source S^{col} . This effect is strongest for the small medium. All four images were put on the same gray scale as figure (2) for direct comparison. The use of a collimated source instead of a diffuse source as in the previous example shows that the anisotropy has to be taken into account for light propagation in tissue for small geometries such as $1\text{cm} \times 1\text{cm}$ and $2\text{cm} \times 2\text{cm}$.

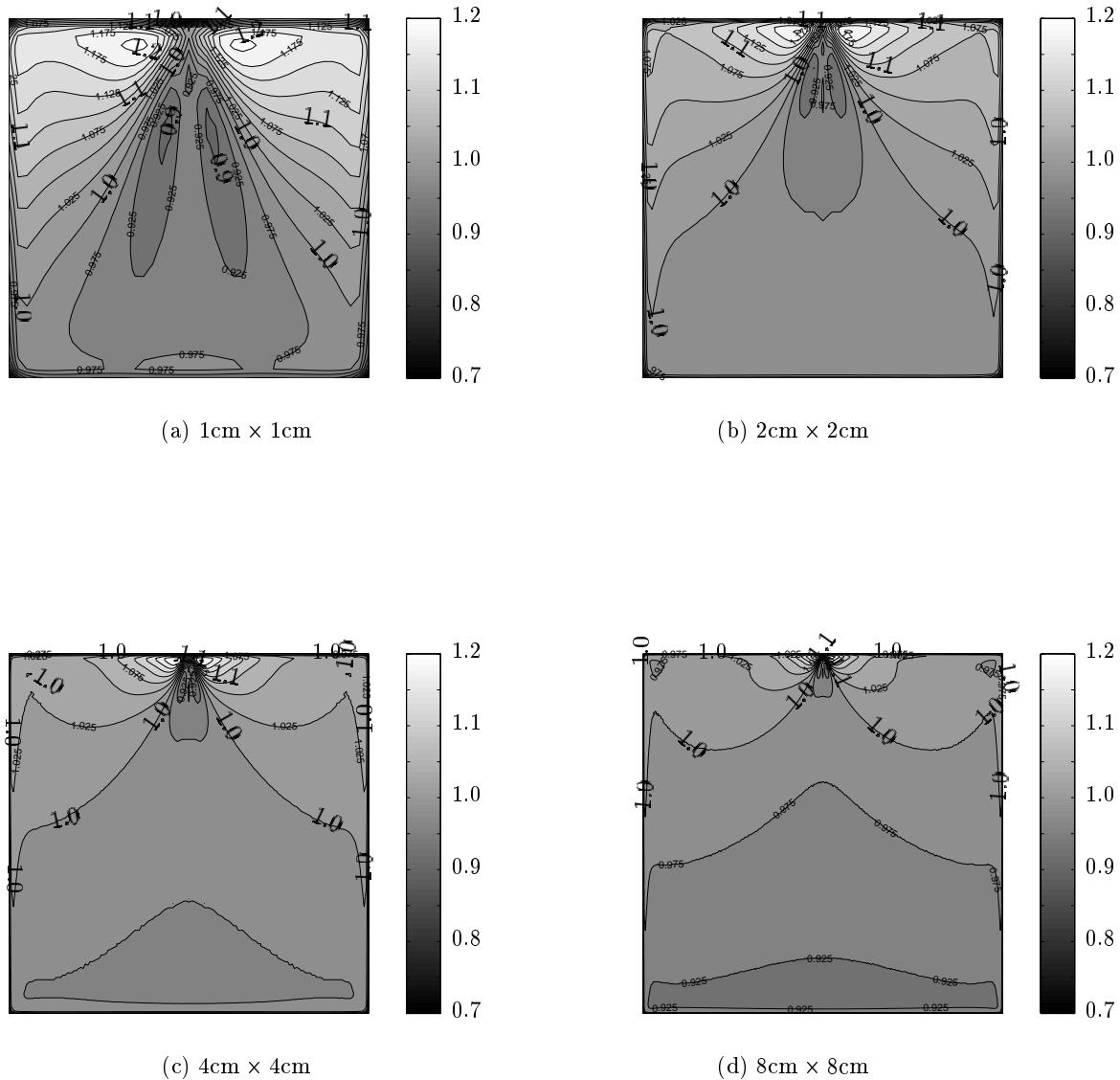


Figure 3. Ratios $\phi^{g=0.95}/\phi^{g=0}$ for different media sizes: (a) $1\text{cm} \times 1\text{cm}$, (b) $2\text{cm} \times 2\text{cm}$, (c) $4\text{cm} \times 4\text{cm}$, (d) $8\text{cm} \times 8\text{cm}$. A collimated source was placed at the top center of the medium boundary.

3.4. Isotropically Scattering Media With Different Sources

We calculated the fluence distributions, ϕ^{col} and ϕ^{dif} , in isotropically scattering media ($g = 0$) for a collimated, S^{col} , and a diffuse, S^{dif} , source. The images in figure (4) depict the ratios ϕ^{col}/ϕ^{dif} for different media sizes. As can be seen in figure (4) the ratios between the light distributions of both sources are in the range between 1.2 to 2.4. It is highest in the vicinity of the source position. This effect is largest for the smallest medium with $1\text{cm} \times 1\text{cm}$.

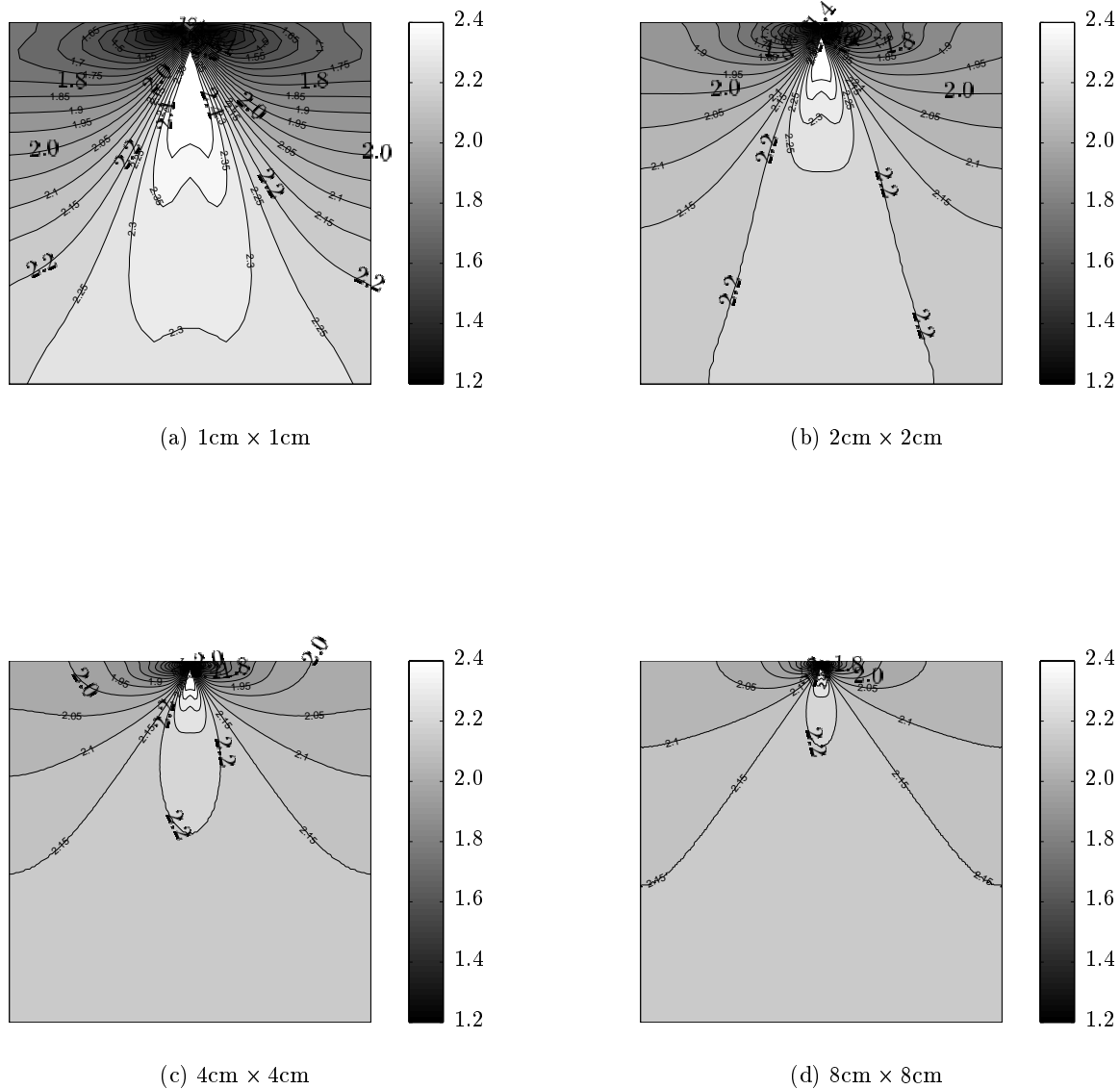


Figure 4. Ratios ϕ^{col}/ϕ^{dif} for different media sizes: (a) $1\text{cm} \times 1\text{cm}$, (b) $2\text{cm} \times 2\text{cm}$, (c) $4\text{cm} \times 4\text{cm}$, (d) $8\text{cm} \times 8\text{cm}$. The collimated, S^{col} , or diffuse, S^{dif} , source was placed at the top center of the medium boundary. The medium had an anisotropy factor $g = 0$. An up to 140 % higher fluence ϕ^{col} is observed due to the collimated source since more light energy is deposited into the medium.

3.5. Anisotropically Scattering Media With Different Sources

In the last example we calculated the fluence distributions, ϕ^{dif} and ϕ^{col} , for a diffuse source S^{dif} and a collimated source S^{col} in anisotropically scattering media with $g = 0.95$ instead of an isotropically scattering medium as in the previous example. The images in figure (5) show the ratios of fluence distributions. All images are displayed at the same gray scale as in figure (4) for better comparison. We found similar results as in the previous example for isotropically scattering media.

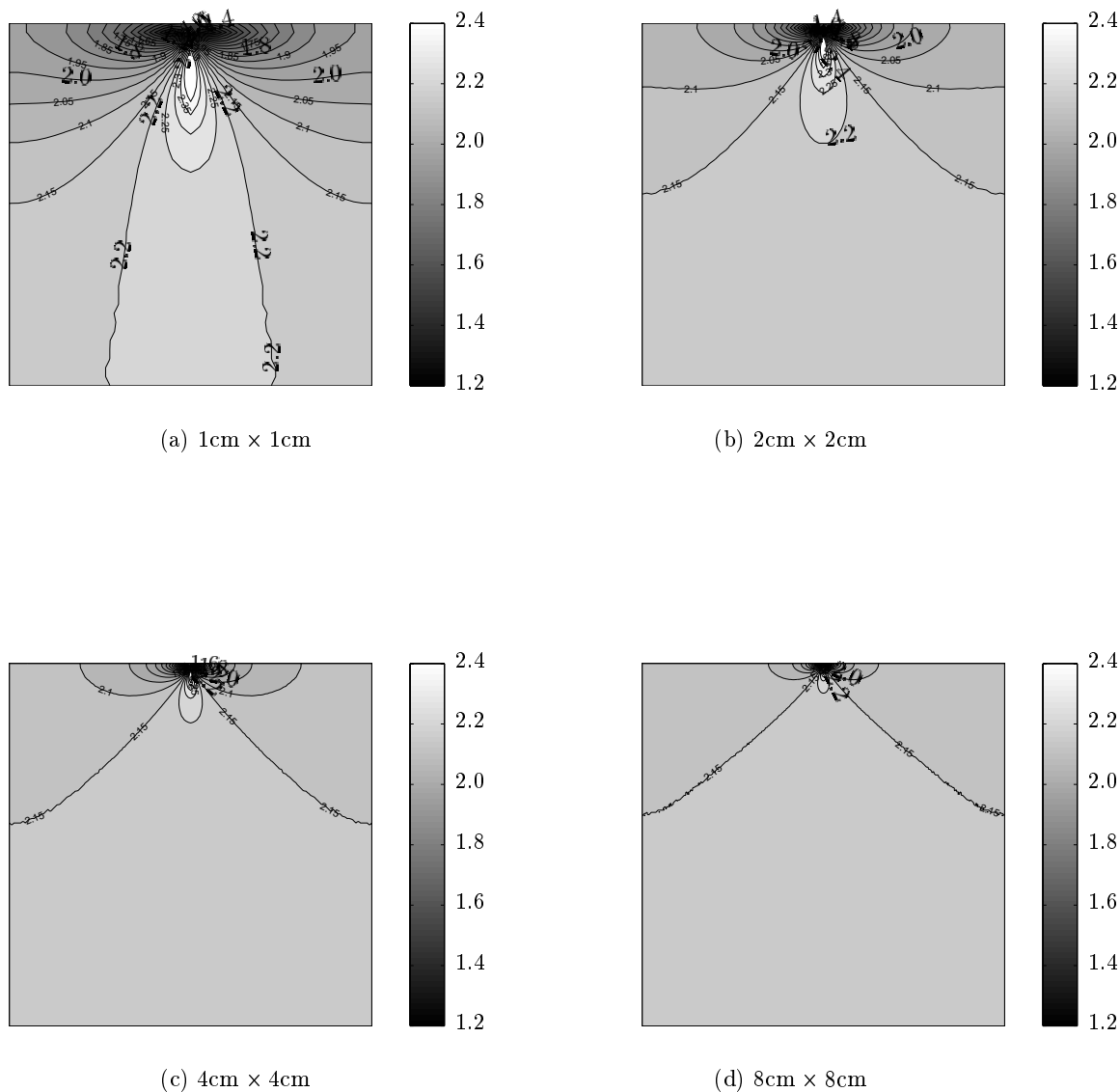


Figure 5. Ratios ϕ^{col}/ϕ^{dif} for different media sizes: (a) 1cm × 1cm, (b) 2cm × 2cm, (c) 4cm × 4cm, (d) 8cm × 8cm. The collimated or diffuse source was placed at the top center of the medium boundary. The medium had an anisotropy factor $g = 0.95$. A larger fluence ϕ^{col} is observed for the collimated source due to the higher source power density at forward directions.

4. CONCLUSION

We have implemented a Delta-Eddington method in conjunction with a finite-difference discrete-ordinates technique to solve the equation of radiative transfer in highly scattering media. The Delta-Eddington method reduces the number of discrete ordinates used for the angular discretization. The numerical solution can be calculated with less computational effort. Thus, highly anisotropically scattering media ($g > 0.8$) could be studied.

The light propagation in anisotropically scattering media was compared to the light propagation in isotropically scattering media for different medium sizes. In addition, diffuse and collimated sources were considered. We found minor discrepancies for media with dimensions larger than 20 mean free reduced scattering lengths ($20 \mu'_s{}^{-1}$) when diffuse sources were present. For media with dimensions around 10 mean free reduced scattering lengths ($10 \mu'_s{}^{-1}$) a deviation of 20 % between the light distributions of the isotropically and anisotropically scattering medium and collimated sources could be found. In the case of direct comparison of collimated and diffuse sources the error between both light distributions can be larger than 100 %. The largest deviations are present in the vicinity of the source.

We conclude from the performed numerical study that both the anisotropy factor g and the scattering coefficient μ_s instead of the reduced scattering coefficient $\mu'_s = (1 - f)\mu_s$ has to be taken into account for small tissue geometries when collimated sources are present in order to obtain sufficiently accurate results. The results are of particular importance for optical imaging of finger joints and molecular imaging of small animals.

ACKNOWLEDGMENTS

We thank Dr. Guillaume Bal at the Department of Applied Mathematics, Columbia University New York, for fruitful discussions on scattering phase functions. This work was supported in part by a postdoctoral fellowship for Alexander D. Klose from the Ernst-Schering Research Foundation (Germany), and the National Institute of Arthritis and Musculoskeletal and Skin Diseases (NIAMS - grant # R01 AR46255).

REFERENCES

1. S. R. Arridge, "Optical tomography in medical imaging," *Inv. Prob.* **15**, pp. R41–R93, 1999.
2. A. H. Hielscher, A. D. Klose, and K. M. Hanson, "Gradient-based iterative image reconstruction scheme for time-resolved optical tomography," *IEEE Trans. Med. Imag.* **18(3)**, pp. 262–271, 1999.
3. S. Fantini, M. A. Franceschini, and E. Gratton, "Effective source term in the diffusion equation for photon transport in turbid media," *Appl. Opt.* **36(1)**, pp. 156–163, 1997.
4. A. H. Hielscher, R. E. Alcouffe, and R. L. Barbour, "Comparison of finite-difference transport and diffusion calculations for photon migration in homogeneous and heterogeneous tissues," *Phys. Med. Biol.* **43**, pp. 1285–1302, 1998.
5. A. D. Kim and A. Ishimaru, "Optical diffusion of continuous-wave, pulsed, and density waves in scattering media and comparisons with radiative transfer," *Appl. Opt.* **37(22)**, pp. 5313–5319, 1998.
6. V. Venugopalan, J. S. You, and B. J. Tromberg, "Radiative transport in the diffusion approximation: An extension for highly absorbing media and small source-detector separations," *Phys. Rev. E* **58(2)**, pp. 2395–2407, 1998.
7. R. Aronson and N. Corngold, "Photon diffusion coefficient in an absorbing medium," *J. Opt. Soc. Am. A* **16(5)**, pp. 1066–1071, 1999.
8. T. Spott and L. O. Svaasand, "Collimated light sources in the diffusion approximation," *Appl. Opt.* **39(34)**, pp. 6453–6465, 2000.
9. B. Chen, K. Stamnes, and J. J. Stamnes, "Validity of the diffusion approximation in bio-optical imaging," *Appl. Opt.* **40(34)**, pp. 6356–6366, 2001.
10. Z. Guo and S. Kumar, "Equivalent isotropic scattering formulation for transient short-pulse radiative transfer in anisotropic scattering planar media," *Appl. Opt.* **39(24)**, pp. 4411–4417, 2000.
11. J. J. Duderstadt and W. R. Martin, *Transport theory*, John Wiley & Sons, New York, 1979.
12. E. E. Lewis and W. F. Miller, *Computational Methods of Neutron Transport*, John Wiley & Sons, New York, 1984.

13. B. G. Carlson and K. D. Lathrop, "Transport Theory - The Method of Discrete Ordinates," in *Computing Methods in Reactor Physics*, H. Greenspan, ed., pp. 166–266, Gordon and Breach, New York, 1968.
14. A. D. Klose and A. H. Hielscher, "Iterative reconstruction scheme for optical tomography based on the equation of radiative transfer," *Med. Phys.* **26** (8), pp. 1698–1707, 1999.
15. A. D. Klose, U. Netz, J. Beuthan, and A. H. Hielscher, "Optical tomography using the time-independent equation of radiative transfer. Part I: Forward model," *J. Quant. Spectrosc. Radiat. Transf.* **72**(5), pp. 691–713, 2002.
16. A. D. Klose and A. H. Hielscher, "Fluorescence tomography with simulated data based on the equation of radiative transfer" *Opt. Lett.*, in print, 2003.
17. R. A.J. Groenhuis, H. A. Ferwerda, and J. J. Ten Bosch, "Scattering and absorption of turbid materials determined from reflection measurements. 1: Theory," *Appl. Opt.* **22**(16), pp. 2456–2462, 1983.
18. S. A. Prahl, M. J.C. van Gemert, and A. J. Welch, "Determining the optical properties of turbid media by using the adding-doubling method," *Appl. Opt.* **32**(4), pp. 559–568, 1993.
19. L. H. Liu, L. M. Ruan, and H. P. Tan, "On the discrete ordinates method for radiative heat transfer in anisotropically scattering media," *Int. J. Heat Mass. Transf.* **45**, pp. 3259–3262, 2002.
20. J. H. Joseph, W. J. Wiscombe, and J. A. Weinman, "The delta-Eddington approximation for radiative transfer," *J. Atmos. Sci.* **33**, pp. 2452–2459, 1976.
21. B. H.J McKellar and M. A. Box, "The scaling group of the radiative transfer equation," *J. Atmos. Sci.* **38**, pp. 1063–1068, 1981.
22. A. H. Hielscher and R. E. Alcouffe, "Discrete-ordinates transport simulations of light propagation in highly forward scattering heterogeneous media," in *OSA TOPS Vol 21 Advances in Optical Imaging and Photon Migration*, J. G. Fujimoto and M. S. Patterson, eds., pp. 23–28, Optical Society of America, Washington DC, 1998.